POLITECNICO MILANO 1863

SCUOLA DI INGEGNERIA INDUSTRIALE E DELL'INFORMAZIONE

EXECUTIVE SUMMARY OF THE THESIS

Free space optical systems simulator in turbulent propagation regime

LAUREA MAGISTRALE IN TELECOMMUNICATION ENGINEERING - INGEGNERIA DELLE TELECOMUNICAZIONI

Author: MARCO GHIGI

Advisor: PROF. ANDREA IVANO MELLONI

Co-advisor: ANDRES IVAN MARTINEZ ROJAS

Academic year: 2022-2023

---

1. Introduction

Free Space Optical (FSO) communication systems present remarkable benefits for data transmission over long distances, largely attributed to their high optical bandwidth and bit rate capabilities. A salient advantage that sets FSO systems apart from conventional Radio Frequency (RF) systems is their narrower beam divergence. This property leads to enhanced directional precision and security, mitigating the potential for signal interception and interference.
FSO systems , however, present many challenges, atmospheric turbulence being the primary one. A random process resulting from temperature and pressure fluctuations in the atmosphere. These fluctuations cause significant performance degradation in FSO systems. While various mitigation strategies exist, effectively overcoming the impact of atmospheric turbulence remains a complex issue.
To solve this problem we develop simulator that accurately models the propagation of beams through turbulence. This simulator has been adjusted and fine-tuned to accurately generate turbulence induced effects on beams of any shape and dimension.
An innovative downscaling option is presented, which enables the simulation of the effects of an outdoor scenario on a beam to be reproduced on a smaller beam over a reduced propagation distance. Furthermore, we expand our research to incorporate optical functions that permit beam tilting and lensing, both within the simulator and for programming matrices for a Spatial Light Modulator (SLM). In addition to this, we have devised a function for creating phase masks and forked gratings for an SLM designed to transition light from the fundamental mode to higher-order Gaussian modes.

2. Atmospheric turbulence

Simulating an FSO system presents three main challenges:

- **Divergence:** Beam divergence plays a significant role in the geometric losses in the channel because of the beam expansion (Figure 1). For instance, a beam with a waist $w_0 = 0.4\,mm$ can extend to $w = 2\,m$ after a propagation distance of $z = 800\,m$. Therefore in a simulation, we must adequately sample the initial beam and prevent the final beam from wrapping around the simulation region and cause aliasing. Thus the simulation region must change dynamically with the propagating beam size.

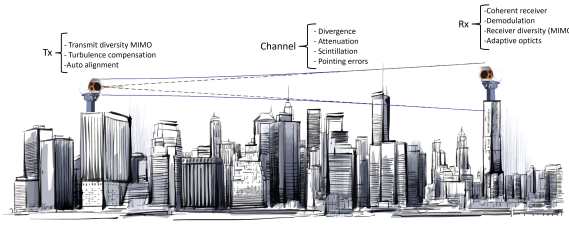

Figure 1: Illustration of a Free Space Optics (FSO) system.

- **Phase sampling:** The computational representation of the Fresnel integral includes a "chirp" function, a phase term that increases quadratically with frequency. The sampling of this chirp function poses a challenge in a propagation simulation, primarily because the phase slope progressively escalates with frequency [2].
- **Turbulence:** Turbulence causes random refractive index inhomogeneities along the transmission path. These random alterations result in regions (Figure 2) that cause fluctuations in intensity and phase of the light beam (Figure 3) .

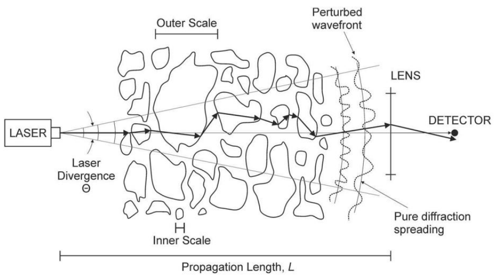

Figure 2: Beam propagating through turbulence. The anisotropic media is represented as cells each one with different refractive index [2]

As a laser beam passes through turbulent zones, two effects occur:

1. Scintillation: random redistribution of the beam energy that causes loss of spatial coherence.
2. Beam wander: unpredictable temporal shifts in the beam's centroid position.

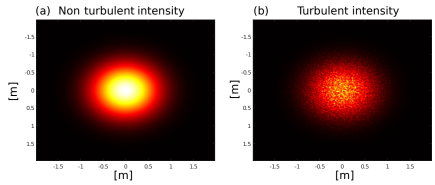

Figure 3: Effect of turbulence on beam intensity
.

To quantify the effects of turbulence on a light beam the Fried parameter , r_0, is commonly used. This parameter indicates the radius of a circle that determines the phase coherence of the wavefront of a light beam (Figure 4). The ratio d/r_0 between the beam diameter d and r_0 provides information about the turbulence level experienced by the beam.

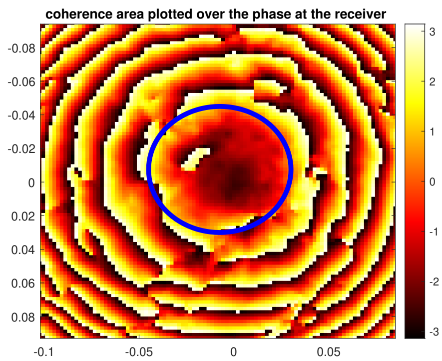

Figure 4: Coherence area of a beam affected by atmospheric turbulence

3. Numerical FSO simulator

In this chapter, we show our simulation methodology for beam propagation, incorporating vital features and the implementation of turbulence. To ensure fidelity of the simulations to real-world outcomes, we undertake a comprehensive convergence study, effectively optimizing the implementation of turbulence within the simulator.

3.1. Beam propagation

The numerical simulator for FSO has been implemented through three progressive iterations: FT propagation, the "Step-by-step" simulator and the Angular Spectrum Propagator. The normalized overlap integral served as the figure of merit for the reliability of the simulator.

- **Fresnel Transfer Function Simulator** implements the Fresnel diffraction integral specifically its transfer function, to propagate the beam[4]. However due to the chirp function present in the beam and the constant simulation region sampling is critical and requires a lot of memory to achieve correct simulation. This causes the beam to wrap around the simulation region leading to aliasing(Figure 5).

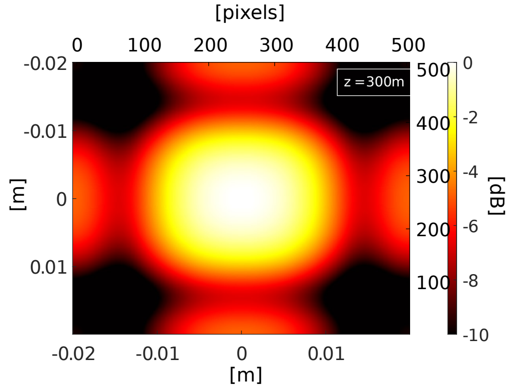

Figure 5: Beam results aliased as the divergence makes the beam wrap around the simulation region

- **"Step-by-Step" Simulator:** This solution solves the divergence problems as after each "step" the beam is down-sampled, and the simulation region size is increased by the same factor. This confines the beam while keeping the number of the pixels constant. To solve the phase sampling the algorithm switches from the Transfer function to the Impulse response interpretations of the Fresnel diffraction integral (Fig.6 shows the algorithm flowchart) . These two approaches yield opposite regimes of undersampling, so when the first would be come aliased the other is correct. The drawback of this approach is that due to the simplistic implementation of down-sampling, the beam loses phase information. This is confirmed performing the overlap integral with an analytically calculated Gaussian beam as it never equals 1.

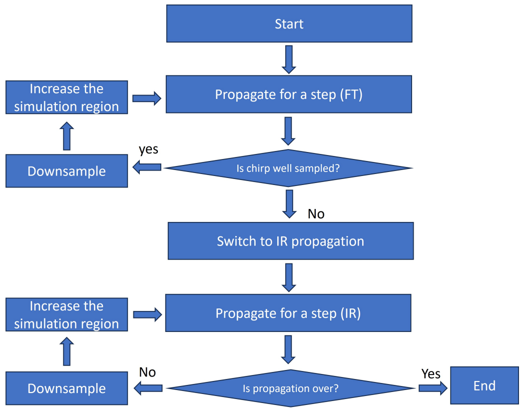

Figure 6: Flowchart of the "Step-by-Step" simulator

- **Angular Spectrum Propagation Simulator** This approach separates a wavefront into its plane wave components, propagates each of them, and reassembles them at the arrival point [3]. We modified this method to include a scaling factor between the initial and final observation planes' sampling interval, this facilitated an adaptive simulation region. With this improvement the simulator can propagate any beam shape with arbitrary waist dimension for any distance, with an overlap with the analytical Gaussian consistently equalling $0dB$. Figure 7 shows a comparison of the normalized overlap between the three simulators and the analytical solution. Simulations were done with an initial beam waist $w_0 = 10\,mm$ at a $\lambda = 1550\,nm$, with an initial simulation region of side length $L = 40mm$.

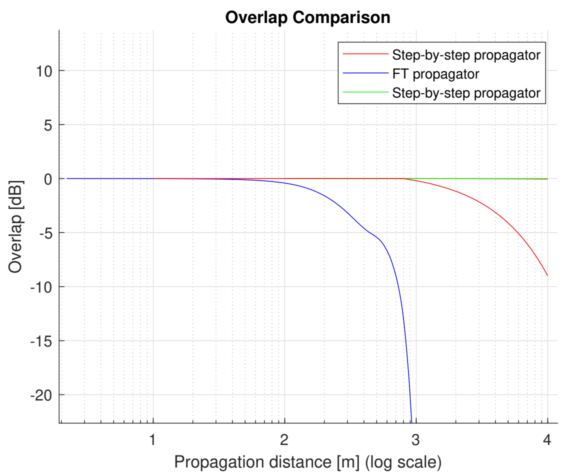

Figure 7: Comparison of overlap values for the three simulators.

3.2. Turbulence emulation

We implemented turbulence using the Split-Step method [1]. This method alternates propagation through free space and a non-diffractive medium , as depicted in figure 9, introducing turbulence via a randomly generated phase screen using the Von Karman model.

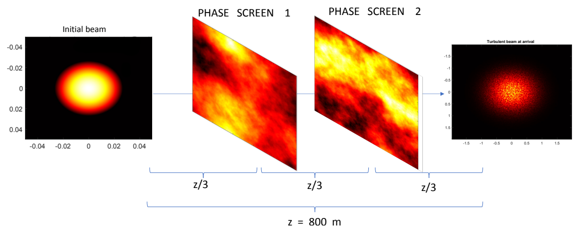

Figure 8: Split-Step Method

A study of convergence was conducted to determine the requisite number of phase screens to accurately model turbulence for a given scenario. To ensure consistency we use a set of 800 correlated phase screens. The process is depicted in figure 9, each iteration a fixed number of phase screen is extracted from the set and the beam is propagated with the Split-Step method through them. The results of the integrated power on an area of $1\,cm^2$ are then saved in an array, so that after many (100 in our case) simulations we can study the expected value and the standard deviation of the power distribution and confront these results with the ones coming from simulations with a different number of phase screens. In the case of the scheme the simulation is issued with two phase screens for each iteration.

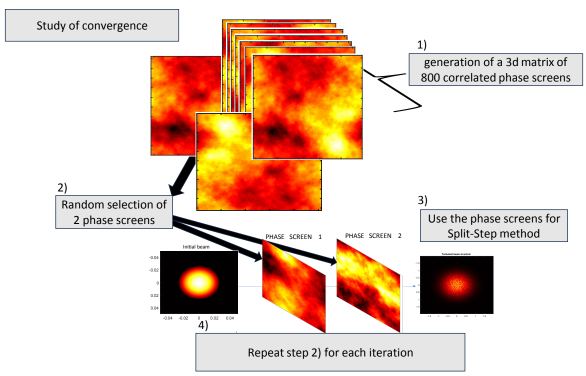

Figure 9: Algorithm for the study of convergence

It was concluded that even a single phase screen suffices in simulating propagation over an $800m$ link with $Cn^2 = 10^{-14}\left[\mathrm{m}^{-2/3}\right]$, as indicated by the consistent mean and standard deviations values of the power distributions saved from the simulations (table 1).

Phase Screens	Mean Value	Standard Deviation
1	-56.95	1.64
2	-57.23	1.54
4	-56.28	1.40
8	-57.11	1.82

Table 1: Mean value and standard deviation of the distribution of integrated power on $1cm^2$ for different number of phase screens

3.3. Non Gaussian inputs

The strength of this simulator also lies in its capability to propagate non-Gaussian input beams, thanks to its method of estimating the simulation region size. This feature is crucial in telecommunications, where arrays of Gaussian beams are commonly used. Studying their far-field patterns became feasible thanks to this simulator. The figure 10 showcases two beams, exhibiting fringes in far field pattern, while Fig. 11 the 16-beam array propagating to far-field .

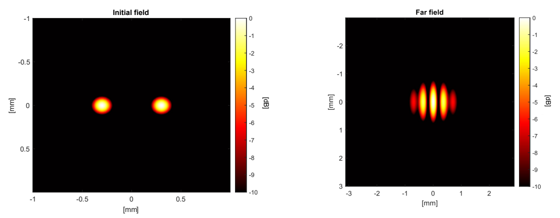

Figure 10: Intensity of Gaussian beams of waist $w_0 = 100\,\mu m$ set $d = 1\,mm$ apart propagating to far field

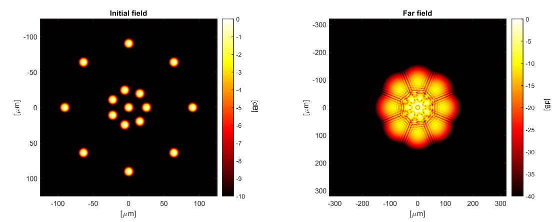

Figure 11: Intensity of Gaussian beams of waist $w_0 = 5\,\mu m$ set on two concentric circles, propagating to far field

4. Additional functionalities

The next step revolves around the augmentation of the simulator with features such as tilt, lensing, and turbulence simulation, with a particular emphasis on downscaling outdoor scenarios to more tractable distances.

4.1. Tilt and lenses

Tilt implementation involved creating specially designed phase ramps, verified by measuring the distance from the center after propagation over a defined distance [4]. In the test a $5\mu m$ is projected at a 30 angle over $10\mu m$, and the resulting distance from the center is precisely $10 \cdot \tan 30 = 5.77\mu m$ confirming the validity of the implementation. Lensing was actualized using lens transmittance functions, similar to the focusing functions incorporated as a fundamental building blocks [4]. The functionality of lensing was validated using a 4f double lens system, which theoretically should output the same intensity pattern as the beam, albeit mirrored both on the horizontal and vertical axes. This is portrayed in Figure 12 where a beam is shone and the symmetry of the output beam shows a vertical and horizontal inversion with respect to the input plane. This is easy to spot because of a "T" shape in the beam intensity that can be used as a point of reference for the symmetry.

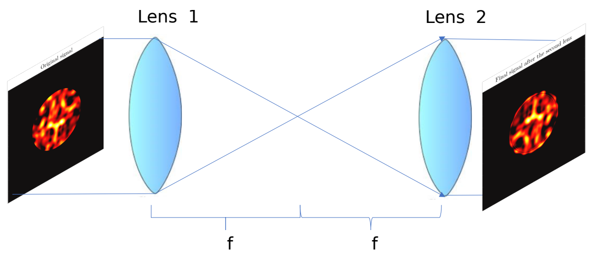

Figure 12: Simulation of a 4f lensing system. Output shows the expected symmetry for the intensity pattern

4.2. Downscaling

The simulator can be used to downscale an outdoor scenario to more manageable distances. The metric used to evaluate this was the d/r_0 ratio, which provides a measure of turbulence experienced by the beam. The same level of turbulence was successfully replicated using a $0.4mm$ beam propagated over $800\,m$ with Cn^2 of $10^{-14}\left[\mathrm{m}^{-2/3}\right]$, and a $3\,mm$ beam simulated through a phase screen with Cn^2 of $10^{-10}\left[\mathrm{m}^{-2/3}\right]$ over just $2\,m$. The final d/r_0 was 24 in both cases confirming the accurate downscaling of the outdoor system. The simulation result is depicted in Figure 13, where the two simulations are put side by side, showing the final consistency of the results.

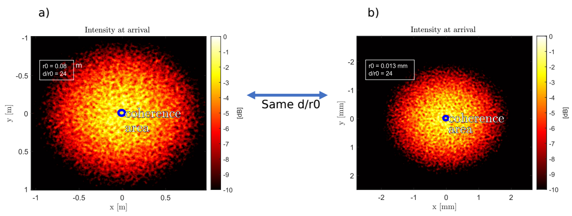

Figure 13: Downscaling simulations, intensity at arrival. The coherence area is plotted over the intensity showing the d/r_0 ratio is the same between the two beams.

4.3. Experimental measurements

This section shows the results obtained from the experiment conducted between "Casa dello studente" and "Building 24", as well as insights from the spatial light modulator (SLM) programmed within the lab. The purpose was to analyze both environments and employ the results to either corroborate the reliability of the simulator or broaden its applications .

5. Rooftop Experiment

The rooftop experiment was conducted over an 800 meter link using a commercial transmitter, "Sona-Beam", that utilized two lasers as sources. The anticipated pattern at far-field consisted in fringes due to the two lasers interfering. This scenario was replicated in the simulator using the superposition theorem to handle the considerable distance between the beams ($8\,cm$) relative to their beam waist ($0.4\,mm$). The beams were then propagated using a Split-Step environment to simulate the turbulent fringes observed at the receiver, which were characterized by turbulence-induced irregularities and fast movements through the camera screen.

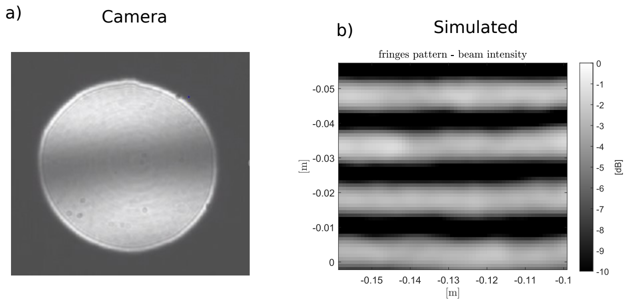

Figure 14: Beam intensity at the receiver. a) shows the real results from the IR camera, b) is the simulation.

For a quantitative analysis, the power of the simulated turbulent beam was integrated over an area comparable to that of the photodiode $1cm^2$in the actual setup. The average power and the standard deviation of the power over a $300s$ measurement were compared, revealing that the results were again congruent (Fig. 15). This result along with the turbulent fringe shape matching the one from the experiment, affirmed the successful simulation of diverging and interfering turbulent beams.

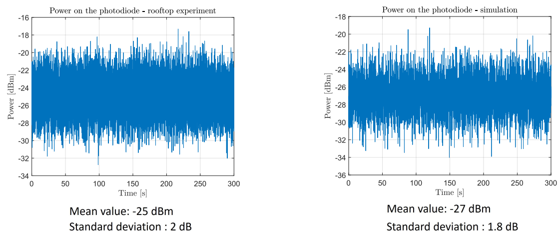

Figure 15: Received optical power the experimental measurments the simulated result

5.1. SLM Programming

The final segment of the project involved programming a Spatial Light Modulator (SLM). An SLM is a versatile tool capable of modifying the phase of incident light on its nematic liquid crystals screen by manipulating its birefringence through the applied electric field.
The initial phase mask applied to the SLM was a matrix computed using the Von Karman function, the reflected light after a $z = 30cm$ path was captured by an IR camera. An identical scenario was simulated with a $w_0 = 3mm$ propagating for $z = 30cm$, and the two turbulent results were compared (Fig. 16). The results demonstrated a similar pattern, thereby indicating that the downscaling demonstrated could be implemented in the lab by applying a higher turbulence phase screen on the SLM.

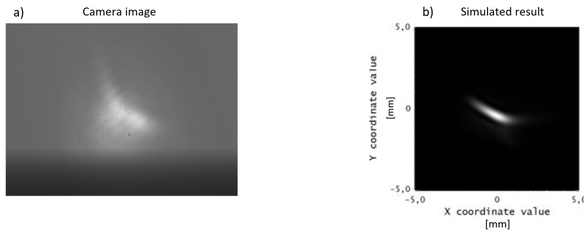

Figure 16: Turbulent beam intensity captured from the camera in the lab and simulated with the same phase screen .

The SLM can also be programmed to implement other functionalities, such as tilt or lenses. Both functionalities were encoded and the generated patterns showcase the incredible versatility of the SLM. Thanks to self implemented functions, the final functionality programmed on the SLM is the generation of patterns to transition from the fundamental mode to higher-order modes, such as HG01 or HG33. Particular attention was given to LG33. The phase pattern was calculated and an apposite forked grating (figure 17) was designed so that only the part of the light that coupled to LG33 was deviated away from the non coupled light. The line spacing in the grating determines the angle of diffraction, that is designed to be higher than the divergence angle of the beam.

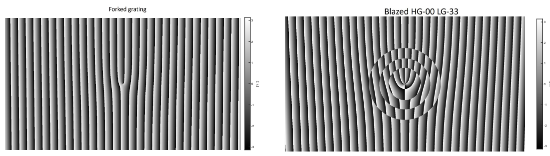

Figure 17: Forked grating with the resulting overlaid phase mask used to separate LG33 light from non-coupled light.

The phase pattern was calculated and uploaded, and the reflected light was captured by the camera, as shown in the figure 18 confirming the fact that the phase pattern were acting as we wanted them.

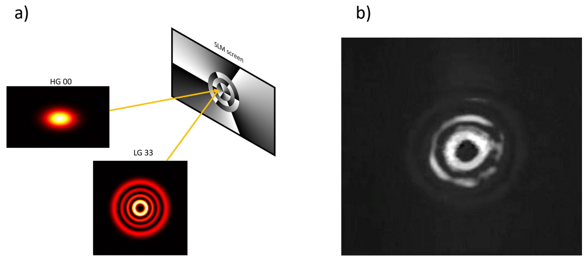

Figure 18: Phase pattern for HG00 - LG33 (a) and reflected light as captured by the camera (b) once the pattern is applied .

18 (a) shows the phase pattern without the forked grating. This is instructive for two reasons: it shows the real needed pattern to obtain LG33 and it illustrates that in a simulation (where all the light gets coupled with the Laguerre Gaussian mode) there is no reason to use the forked pattern.

6. Conclusions

A solution for simulating and manipulating complex beam propagation in Free Space Optics systems was devised, proposing a refined Angular Spectrum propagator. The simulator can propagate any type of beam for any distance with perfect accuracy. ASP is then tested to be accurate if used in the Split-step method so after a study of convergence we estimated one as the number of phase screens needed to simulate the turbulence in this case.
A novel downscaling method was proposed for turbulence calculations, which replicates the effects of turbulence on smaller beams, mimicking those on more divergent beams over longer distances.
The implementation of this turbulence effects in the laboratory was made possible using a Spatial Light Modulator (SLM), explored in detail in this work. The SLM also enables the generation of higher-order Gaussian modes if well programmed, in our case we also had to develop forked grating to separe the higher order gaussian from the rest of the light.

References

[1] Monish R. Chatterjee and Fathi H. A. Mohamed. Split-step approach to electromagnetic propagation through atmospheric turbulence using the modified von Karman spectrum and planar apertures. *Optical Engineering*, 53(12):126107, 2014.

[2] Janusz Mikołajczyk, Zbigniew Bielecki, Maciej Bugajski, Józef Piotrowski, Jacek Wojtas, Waldemar Gawron, Dariusz Szabra, and Artur Prokopiuk. Analysis of free-space optics development. *Metrology and Measurement Systems*, 24:653–674, 12 2017.

[3] J.D. Schmidt. *Numerical Simulation of Optical Wave Propagation with Examples in MATLAB*. Press monograph. SPIE, 2010.

[4] D.G. Voelz. *Computational Fourier Optics: A MATLAB Tutorial*. SPIE Press, 2011.